**Gianmarc Coppola**
Robotics and Automation Laboratory,
University of Ontario Institute of Technology,
Oshawa, ON, L1H 7K4, Canada
e-mail: gianmarc.coppola@uoit.ca

**Dan Zhang**[1]
Robotics and Automation Laboratory,
University of Ontario Institute of Technology,
Oshawa, ON, L1H 7K4, Canada
e-mail: dan.zhang@uoit.ca

**Kefu Liu**
Department of Mechanical Engineering,
Lakehead University,
Thunder Bay, ON, P7B 5E1, Canada
e-mail: kefu.liu@lakeheadu.ca

**Zhen Gao**
Robotics and Automation Laboratory,
University of Ontario Institute of Technology,
Oshawa, ON, L1H 7K4, Canada
e-mail: zhen.gao@uoit.ca

# Design of Parallel Mechanisms for Flexible Manufacturing With Reconfigurable Dynamics

*Reconfigurable robotic systems can enhance productivity and save costs in the ever growing flexible manufacturing regime. In this work, the idea to synthesize robotic mechanisms with dynamic properties that are reconfigurable is studied, and a methodology to design reconfigurable mechanisms with this property is proposed, named reconfigurable dynamics (Re-Dyn). The resulting designs have not only the kinematic properties reconfigurable, such as link lengths, but also properties that directly affect the forces and accelerations, such as masses and inertias. A 2-degree of freedom (DOF) parallel robot is used as a test subject. It is analyzed and redesigned with Re-Dyn. This work also presents the robots forward dynamic model in detail, which includes the force balancing mediums. The connection method is directly utilized for this derivation, which is well suited for multibody dynamics and provides insight for design parameters (DPs). Dynamic performance indices are also briefly discussed as related to the Re-Dyn method. After redesigning the robot, a full simulation is conducted to compare performances related to a flexible manufacturing situation. This illustrates the advantages of the proposed method.* [DOI: 10.1115/1.4024366]

## 1 Introduction

Parallel manipulators (PM) with applications to the manufacturing regime have received much attention in the past two decades [1]. Research and development of parallel manipulators stem mainly from the fact that they have promised advantages over their serial counterparts. These advantages also come with a few trade-offs. One of which is a more complex design and highly nonlinear kinematics and dynamics. These complexities demand new and updated techniques applicable to parallel mechanisms. However, engineering design methodologies for parallel robotic mechanisms are scarce. The field of mechanism synthesis can be in some circumstances extended to the robotic regime. This however, only takes into consideration kinematic properties. In this paper, an engineering design methodology termed Re-Dyn is proposed for the design of reconfigurable parallel robotic mechanisms, specifically for the flexible manufacturing regime.

One important attribute in development of a parallel machine or robot is its dynamic characteristics. Thus, a model of its dynamics, either forward or inverse, is required for subsequent analysis and simulations. However, the algorithms developed for serial robots cannot be easily applied to parallel robots [2], mainly due to the connected constraints that parallel mechanisms have. Attempts at formulating dynamic models in this regime usually come in a few methodological forms. The Newton-Euler method [3] can be applied mainly for inverse dynamic models. Other methods consist of the Lagrange method [4], the method of virtual work [5], Kanes method [6] and the connection method [7], which is another form of the virtual work principle. These methods have been applied to various parallel mechanisms [5,7–11]. In this study, the connection method is directly utilized due to its methodological approach and efficiency at multibody dynamics.

The importance of dynamic performance indices has grown recently [12]. Most studies reveal that parallel manipulators have a large variability of performance with their workspace. Some researchers strive to optimize this to a more uniform performance. Several relevant studies in this area are [1,5,8,9,13–15]. Force balanced mechanisms are also sometimes referred to as reactionless mechanisms. In Ref. [16] reactionless four-bar linkages are studied with particular attention to the input torque needed to operate the mechanism. Also, in Ref. [17] the design of reactionless 3DOF parallel mechanisms is addressed. The 3DOF mechanisms are constructed using individual four-bar mechanisms. In Ref. [18], the static balancing of a Gough/Stewart-Type platform is addressed. Using both elastic elements and counterweights, each leg is balanced. Other relevant studies are given in Refs. [18–25].

The design of mechanisms, particularly the synthesis of mechanisms and robotic mechanisms, has been studied through various methods, most of which stem from linkage synthesis methods, such as graphical linkage synthesis or kinematic synthesis. For example, in Ref. [26] a method is proposed to synthesize adjustable planar and spherical four-bar linkages to a set of positions based on Burmester curves. Using adjustable linkages, the number of solutions for their problem goes to infinity. Also, some iterative methods that cleverly include the design of the control parameters and the mechanical structure together have been investigated. A high speed serial robotic application has been investigated in Ref. [27]. A similar two-link robot was used as a test subject in Ref. [28] where a recursive experimental optimization method was used. The importance of these studies is the incorporation of the control parameters and structure design in the methods in a new way. Also important are the studies that use the design for control method proposed in Ref. [29,30] and the adjustment of kinematic parameter method in Ref. [31]. These are related methods that essentially use the adjustment of some of the mechanism's kinematic parameters, such as link lengths, to provide balancing for the mechanisms. This in turn can result in better control performance, as a balanced mechanism can have a simpler dynamic model.

The idea to synthesize mechanisms for various applications has been researched previously. The breadth of this area is essentially limited to simple mechanisms of 1 DOF such as four-bar mechanisms and its variations as well as many other planar 1-DOF mechanisms. Also, the synthesis methods studied are restricted to varying kinematic properties such as a single links length. Various methods have been proposed in literature such as those by [26,32–34]. In the regime of robotics this type of synthesis is in its early stages, as not a lot of research has been done in this area. It has a large potential to various applications in many regimes.

[1]Corresponding author.

Contributed by the Mechanisms and Robotics Committee of ASME for publication in the Journal of Mechanical Design. Manuscript received October 4, 2011; final manuscript received April 15, 2013; published online May 29, 2013. Assoc. Editor: Ashitava Ghosal.

  

In particular, flexible or sustainable manufacturing will be enhanced by findings in this area. Notably, a tool for designing reconfigurable robotic systems was investigated in Ref. [35].

This study proposes a different approach in the design of parallel robotic mechanisms, particularly for flexible manufacturing systems where a proper reconfigurable robotic mechanism is needed. It encompasses a design change to PMs that enables some of their dynamic properties to be reconfigured. In order to appreciate the motivation in accordance with such a method, the regime of mechanism theory must be appropriately understood. In general, the capability of generating multiphase motions or motions that are in accordance with different tasks is highly desirable for industrial applications. This is because industries prefer to utilize the same hardware to fulfill various tasks. This can reduce costs and increase productivity simultaneously. Developing machines, mechanisms and robots that can passively adapt to various tasks is the essence of flexible manufacturing. For example, a mechanism may need to switch its destination between various poses to accommodate different benches or conveyors. An illustration of this can be observed in Fig. 1 using the fundamental four-bar linkage as an example. The simplest and most cost effective way to achieve this is to make one of the links kinematically adjustable in its length. In general, there are three basic types of adjustments; the adjustment to the fixed pivot, moving pivot, or the link length [36]. In the regime of multidegree of freedom mechanisms (robotics), reconfiguration of these same parameters are studied. Notably, between reconfigurations or task spaces much attention has been placed on the kinematic parameters to map design to task. No attention has been given to the performance in terms of forces and accelerations. These dynamic terms however will play a large role in determining the performance and efficiency of the adjustable/reconfigurable robotic system. Consequently, this provides inspiration for the investigation of new methods that can address these dynamic changes between and during different tasks.

Outlined in this manuscript is a systematic approach to synthesizing PMs with reconfigurable dynamics. First, the dynamic design parameters should be properly chosen. This can be done by analyzing the link Jacobian matrices. Then, the functional requirements (FRs) are properly defined in accordance with the flexible requirement of optimally satisfying various operations. Subsequently, the performance criteria are chosen by the designer. Notably, these can even vary between functional requirements. Then, an optimization procedure is conducted treating each FR in parallel with one another. The results of the optimization procedure will yield a multitude of optimal parameters between FRs. It is proposed to utilize the absolute minimum and maximum as bounds for the design parameters to be reconfigured within. The PM can then be physically designed. This proposed procedure is termed Re-Dyn to note its main feature of reconfigurable dynamic properties. In this manuscript, the proposed method is systematically illustrated for a 2DOF parallel robotic structure.

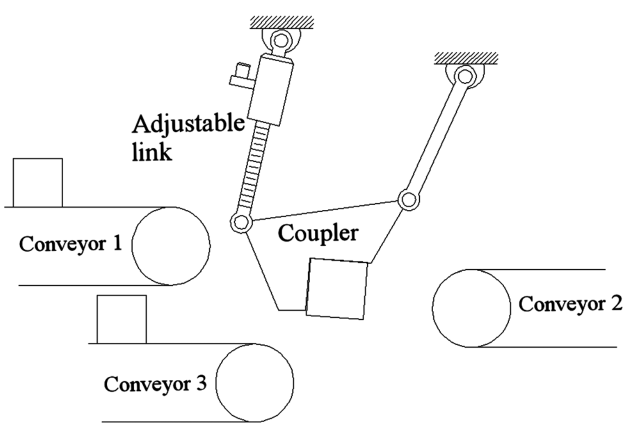


**Fig. 1 Adjustable linkage for flexible manufacturing**

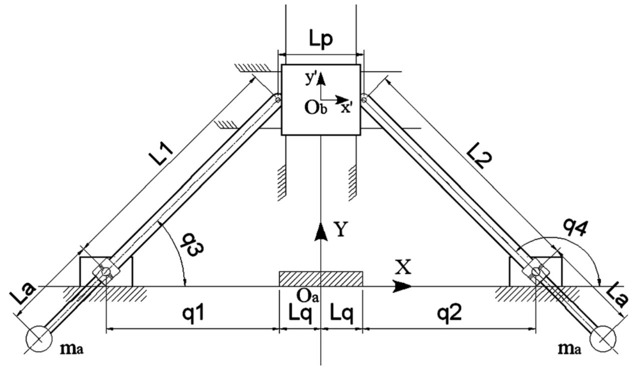


**Fig. 2 Basic structure of the PM (without Re-Dyn)**

The remainder of this manuscript is organized as follows. Firstly, the structure of the robot used as a case study is described. Then, its kinematics and dynamic modeling are described in detail. Subsequently, the dynamic performance and force balancing indices are investigated. Then, the proposed design method is formulated and described while also using the described robotic structure as an example. Finally, in order to illustrate performances, a simulation study is conducted.

## 2 Parallel Manipulator Structure Description

The structure studied in this work is illustrated in Fig. 2. It is composed primarily of a moving platform, two kinematic chains, two prismatic slider joints and counter balancing attachments. Two linear sliders constrain the motion of the parallel mechanism which can more clearly be observed in the conceptual model shown in Fig. 3. All bodies are considered rigid and the gravity is acting in the negative *Y*-direction. The mechanism under consideration is prismatically actuated at its base. The amount of travel of each prismatic actuator is denoted by $q_1$ and $q_2$ in the schematic.

### 2.1 Mobility Via Screw Theory.

In this section, the mobility of the PM used in this study is analyzed. For a complete description of computing the mobility of PMs using this method the reader can refer to Ref. [37].

Referring to Fig. 4, the motion screws of each limb can be formulated. For one of the limbs, this is given by

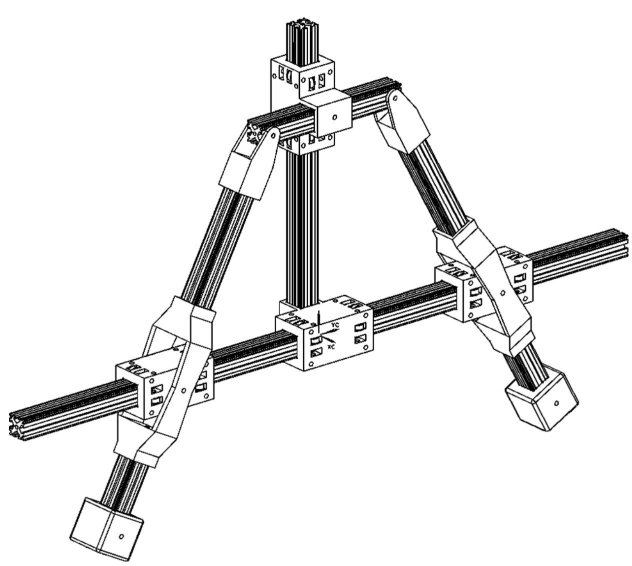

**Fig. 3 Conceptual model of the PM**

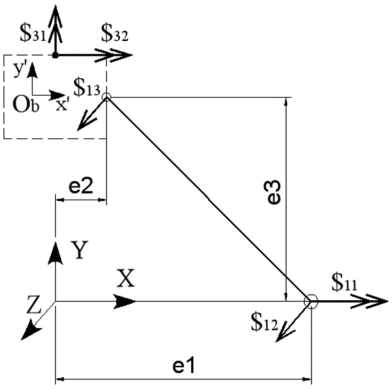


**Fig. 4 Motion screw representation**

$$\$_1 = \left\{ \begin{array}{l} \$_{11} = [0 \quad 0 \quad 0 \quad 1 \quad 0 \quad 0]^T \\ \$_{12} = [0 \quad 0 \quad 1 \quad 0 \quad -e_1 \quad 0]^T \\ \$_{13} = [0 \quad 0 \quad 1 \quad e_3 \quad e_2 \quad 0]^T \end{array} \right\} \tag{1}$$

to which its branch constraint screws can be obtained by taking the reciprocal of Eq. (1). A basis for the reciprocal screws of Eq. (1) is given by

$$\$_1^r = \left\{ \begin{array}{l} [0 \quad 0 \quad 1 \quad 0 \quad 0 \quad 0]^T \\ [0 \quad 0 \quad 0 \quad 0 \quad 1 \quad 0]^T \\ [0 \quad 0 \quad 0 \quad 1 \quad 0 \quad 0]^T \end{array} \right\} \tag{2}$$

Similarly, for the other limb, one can obtain the same constraint screw system as in Eq. (2). This indicates that the two limbs apply the same constraints to the platform. The remaining two screws correspond to the two linear sliders that constrain the motion of the PM. The linear sliders are indicted by the constraint lines in Fig. 2 and are more clearly observed in the conceptual model of the PM in Fig. 3. These can be modeled in the same fashion as above. That is, $\$_{31} = [0 \quad 0 \quad 0 \quad 0 \quad 1 \quad 0]^T$ and $\$_{32} = [0 \quad 0 \quad 0 \quad 1 \quad 0 \quad 0]^T$, to which the constraint screws can be evaluated and amalgamated with the branch constraint screws to form the following platform constraint screw system

$$\$^r = \left\{ \begin{array}{l} [0 \quad 0 \quad 1 \quad 0 \quad 0 \quad 0]^T \\ [0 \quad 0 \quad 0 \quad 1 \quad 0 \quad 0]^T \\ [0 \quad 0 \quad 0 \quad 0 \quad 1 \quad 0]^T \\ [0 \quad 0 \quad 0 \quad 0 \quad 0 \quad 1]^T \end{array} \right\} \tag{3}$$

Finally, the platform motion screws are obtained by taking the reciprocal of Eq. (3). This is given by

$$\$^f = \left\{ \begin{array}{l} [0 \quad 0 \quad 0 \quad 0 \quad 1 \quad 0]^T \\ [0 \quad 0 \quad 0 \quad 1 \quad 0 \quad 0]^T \end{array} \right\} \tag{4}$$

which indicates that the moving platform can translate in the $X$ and $Y$ directions only. Consequently, the mechanism has 2 degrees of freedom.

## 3 Kinematics of the PM

In this section, the robotic structures kinematics is presented. This is essential to the use of such a PM as a case study later in the manuscript. Reference for the kinematics of the unbalanced nominal manipulator used as a case study in this manuscript can be found in Refs. [7,38].

**3.1 Forward and Inverse Kinematics.** In the deduction of the forward and inverse kinematics, it is convenient to introduce the following coordinate systems. The first coordinate system is the fixed Cartesian coordinate, $O_a - XY$, system at the base of the structure as seen in Fig. 2. The second is the moving coordinate system that is fixed to the center of the moving platform denoted $O_b - x'y'$. Let the position vector of the origin $O_b = [x, y]^T$. Subsequently, position vectors connecting the fixed frame to the moving frame can be deduced and solved. A diagram of these position vectors can be seen in Fig. 5. Based on this figure, the following vector loop equation can be written:

$$\hat{R}_t = \hat{u}_1 + \hat{u}_3 + \hat{u}_5 \tag{5}$$

Accordingly, Eq. (5) can be solved and the forward kinematics of this mechanism is given by

$$x = \frac{1}{2}(q_2 - q_1) \tag{6a}$$

$$y = \frac{1}{2}\sqrt{4L_e^2 - Q^2} \tag{6b}$$

where $L = 2L_q - L_p, Q = L + q_1 + q_2$. Also, in this manuscript the lengths of the links along the vectors $\hat{u_3}$ and $\hat{u_4}$ are taken to be equal. That is $L_e = L_2 = L_1$. However, some of the following relations will still differentiate between these lengths for generality of the equations.

The coordinate transformation from joint space to Cartesian space is given by $[q_1, q_2]^T \rightarrow [x, y]^T$. Successively, the inverse kinematics of the mechanism is formulated by solving Eq. (6) for the joint variables. This is given by

$$q_1 = -x - \frac{L}{2} \pm \sqrt{L_1^2 - y^2} \tag{7a}$$

$$q_2 = x - \frac{L}{2} \pm \sqrt{L_2^2 - y^2} \tag{7b}$$

in which the $\pm$ indicates different working modes. Replacing it with a $+$ sign yields the inverse kinematics for the real working case.

**3.2 Jacobian Matrices.** In this subsection, the Jacobian matrices that relate the velocity of the end effector to the velocities of the active joint variables are illustrated. Taking the time derivative of Eq. (6) yields

$$\dot{x} = \frac{1}{2}(\dot{q}_2 - \dot{q}_1) \tag{8a}$$

$$\dot{y} = \frac{-Q}{2\sqrt{4L_e^2 - Q^2}}(\dot{q}_2 + \dot{q}_1) \tag{8b}$$

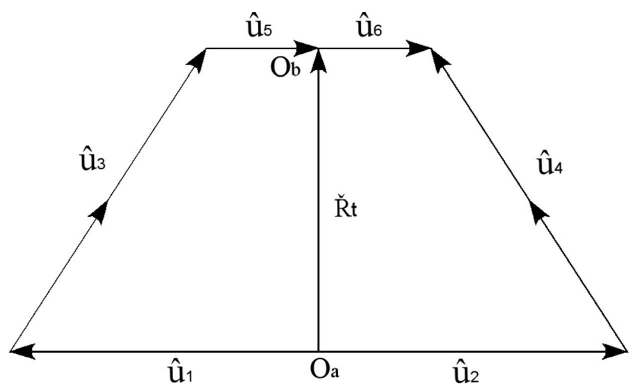


**Fig. 5 Vector diagram of the manipulator**

Taking the velocity of the end effector as $\dot{X} = [\dot{x}, \dot{y}]^T$ and the velocity of the active joint variables as $\dot{q}_a = [\dot{q}_1, \dot{q}_2]^T$ Eq. (8) can be written as

$$\dot{X} = J_q \dot{q}_a \tag{9}$$

where the forward Jacobian matrix is

$$J_q = \begin{bmatrix} -1/2 & 1/2 \\ \dfrac{-Q}{2\sqrt{4L_e^2 - Q^2}} & \dfrac{-Q}{2\sqrt{4L_e^2 - Q^2}} \end{bmatrix} \tag{10}$$

Differentiating Eq. (7) with respect to time yields the relationship

$$\dot{q}_1 = -\dot{x} - \frac{y\dot{y}}{\sqrt{L_1^2 - y^2}} \tag{11a}$$

$$\dot{q}_2 = \dot{x} - \frac{y\dot{y}}{\sqrt{L_2^2 - y^2}} \tag{11b}$$

Equation (11) can be written in the form

$$\dot{q}_a = J_x \dot{X} \tag{12}$$

where the inverse Jacobian matrix is defined as

$$J_x = \begin{bmatrix} -1 & \dfrac{-y}{\sqrt{L_1^2 - y^2}} \\ 1 & \dfrac{-y}{\sqrt{L_2^2 - y^2}} \end{bmatrix} \tag{13}$$

## 4 Dynamics With the Connection Method

This section focuses on the development of a forward dynamic model for the parallel robot under study. Dynamic modeling by the connection method was first proposed by Ref. [7]. It consists essentially of a method that is based on the virtual work principle.

Prior to the formulation of the dynamic model in compact form with the connection method, preliminary expressions of constraints, active and passive matrices must be developed.

**4.1 Active and Passive Constraints.** The relations constraining the active and passive joint variables can be derived from the vector loop equation

$$\hat{u}_2 = \hat{u}_1 + \hat{u}_3 + \hat{u}_5 + \hat{u}_6 - \hat{u}_4 \tag{14}$$

From Eq. (14), the vertical and horizontal components yield the two constraint equations

$$L_1 \sin(q_3) - L_2 \sin(q_4) = 0 \tag{15a}$$

$$L_1 \cos(q_3) - L_2 \cos(q_4) - q_1 - q_2 + L_p - 2L_q = 0 \tag{15b}$$

Thus, the passive joint variables can be expressed by the active joint variables as

$$\cos(q_3) = \frac{q_1 + q_2 + 2L_q - L_p}{2L_1} \tag{16a}$$

$$\cos(q_4) = -\frac{q_1 + q_2 + 2L_q - L_p}{2L_2} \tag{16b}$$

Differentiating Eq. (16) with respect to time yields

$$\dot{q}_3 = \frac{-\dot{q}_1 - \dot{q}_2}{2L_e \sin(q_3)} \tag{17a}$$

$$\dot{q}_4 = \frac{\dot{q}_1 + \dot{q}_2}{2L_e \sin(q_3)} \tag{17b}$$

which can be written in the form directly relating active variables to passive variables

$$\dot{q}_p = J_a \dot{q}_a \tag{18}$$

where

$$J_a = \begin{bmatrix} -\dfrac{1}{2}\dfrac{1}{\sin(q_3)L_e} & -\dfrac{1}{2}\dfrac{1}{\sin(q_3)L_e} \\ \dfrac{1}{2}\dfrac{1}{\sin(q_3)L_e} & \dfrac{1}{2}\dfrac{1}{\sin(q_3)L_e} \end{bmatrix} \tag{19}$$

and $\dot{q}_p = [\dot{q}_3, \dot{q}_4]^T, \dot{q}_a = [\dot{q}_1, \dot{q}_2]^T$.

Subsequently, as defined by the connection method, the active matrix $E_a$ and the passive matrix $E_p$ are defined to separate the joint variables into active and passive joint variables.

$$\text{Let, } E_a = \begin{bmatrix} 1 & 0 \\ 0 & 1 \\ 0 & 0 \\ 0 & 0 \end{bmatrix} \text{ and } E_p = \begin{bmatrix} 0 & 0 \\ 0 & 0 \\ 1 & 0 \\ 0 & 1 \end{bmatrix}$$

The transform velocity matrix from active joint velocities to the generalized variables is now given by

$$J_e = E_a + E_p J_a = \begin{bmatrix} 1 & 0 \\ 0 & 1 \\ -\dfrac{1}{2}\dfrac{1}{\sin(q_3)L_e} & -\dfrac{1}{2}\dfrac{1}{\sin(q_3)L_e} \\ \dfrac{1}{2}\dfrac{1}{\sin(q_3)L_e} & \dfrac{1}{2}\dfrac{1}{\sin(q_3)L_e} \end{bmatrix} \tag{20}$$

**4.2 Dynamic Model.** The next step in formulating the forward dynamic model using the connection method is to establish the link Jacobian matrices that define the constraints on the velocities of the rigid bodies in the connected dynamic system. Presuming that the robotic system is connected by holonomic constraints [7], the kinematic analysis of its rigid bodies can yield a set of constraint equations in a general form

$$F_j(x_i, q) = 0 \tag{21}$$

with

$$(i = 1, 2, \ldots, K, j = 1, 2, \ldots, N)$$

where $N$ is the number of elements in the $i$th link, $K$ is the total number of links, $F_j$ is the implicit function for the $i$th link variable where the terms $x_i$ are the coordinates of the $i$th link described with respect to the base frame $x_i = [x_{i1}, x_{i2}, \ldots, x_{iN}], x_i \in \Re^N$ where $q$ is a set of generalized variables in the joint space, $q = [q_1, q_2, \ldots, q_M]^T q \in \Re^M$. $M$ is the total number of joint variables

The link Jacobian is obtained by analyzing the partial differential of the constraint equation (21) which yields an equation in the familiar form

$$\dot{x}_i = J_i(q)\dot{q} \tag{22}$$

to which interest in dynamic modeling is the Jacobian matrix of the $i$th rigid link. Its general form can be obtained as

$$J_i(q) = \begin{bmatrix} \dfrac{\partial F_1}{\partial q_1} & \cdots & \dfrac{\partial F_1}{\partial q_M} \\ \vdots & \cdots & \vdots \\ \dfrac{\partial F_N}{\partial q_1} & \cdots & \dfrac{\partial F_N}{\partial q_M} \end{bmatrix} \tag{23}$$

Subsequently, the following relation can determine the differential Jacobian matrix of the $i$th link

$$\dot{J}_i(q) = \sum_{k=1}^{M} \dot{q}_k \Gamma_k(q) \tag{24}$$

where

$$\Gamma_k(q) = \begin{bmatrix} \dfrac{\partial^2 F_1}{\partial q_k \partial q_1} & \dfrac{\partial^2 F_1}{\partial q_k \partial q_2} & \cdots & \dfrac{\partial^2 F_1}{\partial q_k \partial q_M} \\ \dfrac{\partial^2 F_2}{\partial q_k \partial q_1} & \dfrac{\partial^2 F_2}{\partial q_k \partial q_2} & \cdots & \dfrac{\partial^2 F_2}{\partial q_k \partial q_M} \\ \cdots & \cdots & \cdots & \cdots \\ \dfrac{\partial^2 F_N}{\partial q_k \partial q_1} & \dfrac{\partial^2 F_N}{\partial q_k \partial q_2} & \cdots & \dfrac{\partial^2 F_N}{\partial q_k \partial q_M} \end{bmatrix} \tag{25}$$

The above formulation is essential to the connection method. The link Jacobian matrices for the studied PM can be derived and are given by

$$J_1 = \begin{bmatrix} -1 & 0 & 0 & 0 \\ 0 & 0 & 0 & 0 \\ 0 & 0 & 0 & 0 \end{bmatrix}, \quad J_2 = \begin{bmatrix} 0 & 1 & 0 & 0 \\ 0 & 0 & 0 & 0 \\ 0 & 0 & 0 & 0 \end{bmatrix}$$

$$J_3 = \begin{bmatrix} -1 & 0 & \dfrac{-m_3 L_l + m_a L_a}{m_l}\sin(q_3) & 0 \\ 0 & 0 & \dfrac{m_3 L_l + m_a L_a}{m_l}\cos(q_3) & 0 \\ 0 & 0 & 1 & 0 \end{bmatrix}$$

$$J_4 = \begin{bmatrix} 0 & 1 & \dfrac{m_3 L_l - m_a L_a}{m_l}\sin(q_3) & 0 \\ 0 & 0 & \dfrac{m_3 L_l - m_a L_a}{m_l}\cos(q_3) & 0 \\ 0 & 0 & 0 & 1 \end{bmatrix}$$

$$J_5 = \begin{bmatrix} -1 & 0 & -L_1\sin(q_3) & 0 \\ 0 & 0 & L_1\cos(q_3) & 0 \\ 0 & 0 & 1 & 0 \end{bmatrix}$$

where $m_3 = m_4 = m_i$ which is the mass of the links, $m_a$ is the mass of the counterweight, $m_l = m_i + m_a, L_a$ is the length of the extension to the counterweight, and $L_l = L_1/2$.

Notable is the influence of the counterweights added to the mechanism. Evidently, as the mass center of the links 3 and 4 (corresponding to $\widehat{u_3}$ and $\widehat{u_4}$) get closer to the pivot point, by the inclusion of the added counterweight, the influence of these rigid body Jacobians becomes less and less onto the dynamic model of the entire system. Subsequently, the differential link Jacobian matrices are given by

$$\dot{J}_1 = \dot{J}_2 = \mathrm{zeros}(3,4), \quad \dot{J}_3 = \begin{bmatrix} 0 & 0 & \dfrac{\beta\cos(q_3)}{2L_1\sin(q_3)}(\dot{q}_1 + \dot{q}_2) & 0 \\ 0 & 0 & \dfrac{\beta}{2L_1}(\dot{q}_1 + \dot{q}_2) & 0 \\ 0 & 0 & 0 & 0 \end{bmatrix}$$

$$\dot{J}_4 = \begin{bmatrix} 0 & 0 & \dfrac{-\beta\cos(q_3)}{2L_1\sin(q_3)}(\dot{q}_1 + \dot{q}_2) & 0 \\ 0 & 0 & \dfrac{\beta}{2L_1}(\dot{q}_1 + \dot{q}_2) & 0 \\ 0 & 0 & 0 & 0 \end{bmatrix}$$

$$\dot{J}_5 = \begin{bmatrix} 0 & 0 & \dfrac{\cos(q_3)}{2\sin(q_3)}(\dot{q}_1 + \dot{q}_2) & 0 \\ 0 & 0 & \dfrac{1}{2}(\dot{q}_1 + \dot{q}_2) & 0 \\ 0 & 0 & 0 & 0 \end{bmatrix}$$

where $\beta = (m_3 L_l - m_a L_a)/m_l$.

**4.3 The Compact Dynamic Formulation by the Connection Method.** The connection method is used to dynamically describe a system of connected rigid bodies. The resulting expression is a compact forward dynamic model of the parallel robotic system of the following form:

$$\begin{aligned} &J_e^T\left\{\left(\sum_{i=1}^{K} J_i^T M_i J_i\right) J_e \ddot{q}_a\right\} \\ &+ J_e^T\left(\sum_{i=1}^{K}\left[\left(J_i^T M_i J_i\right) E_p T_a + \left(J_i^T M_i \dot{J}_i\right)\right]\right) J_e \dot{q}_a \\ &+ J_e^T\left\{\sum_{i=1}^{K} J_i^T F_{wi} - \sum_{i=1}^{K} J_i^T F_{\mathrm{applied},i}\right\} = \tau_a \end{aligned} \tag{26}$$

where $M_i$ is the mass matrix for each rigid body which includes both mass properties and inertial properties, $T_a(q) = J_e^{-1} J_a$, $\sum_{i=1}^{K} J_i^T F_{wi}$ represents the Coriolis forces for each rigid body, $F_{\mathrm{applied},i}$ is the vector of externally applied forces to the $i$th body, which includes the forces of gravity, and $\tau_a$ is a vector of the active forces and torques.

## 5 Force Balancing

A mechanism is said to be force balanced if, for any configuration of the mechanism, it does not produce a net reaction force in any direction onto its base structure. Static/force balancing for parallel manipulators is a relatively recent topic of investigation that has wide potential for applications. The incorporation of some sort of balancing into mechanism design, particularly robotic mechanisms, has the potential for several advantages.

**5.1 Force Balancing Principles.** Figure 6 represents a position analysis of the mass centers of each of the rigid bodies of the robotic system used in this study. The total force applied to the robotic mechanism is the time rate change of the linear momentum plus the total gravitational force. This is given by

$$f_0 = -\frac{d}{dt}\left(M_t \dot{R}_t\right) + M_t g \tag{27}$$

where $M_t$ is the total mass of the mechanism, $f_0$ is the total reaction force applied to the system, $\dot{R}_t$ is the velocity of the mass center, and $g$ is the acceleration due to gravity.

From Eq. (27), one can note that there exists a variation in the reaction force when the linear momentum changes. Thus, any change in linear momentum will produce unwanted effects to the surroundings through the base structure and its components. However, this change in momentum can be eliminated if the mass center is motionless for any conspired configuration of the manipulator. This inspires an analysis of the position vector of the mass center. Correspondingly, one can deduce

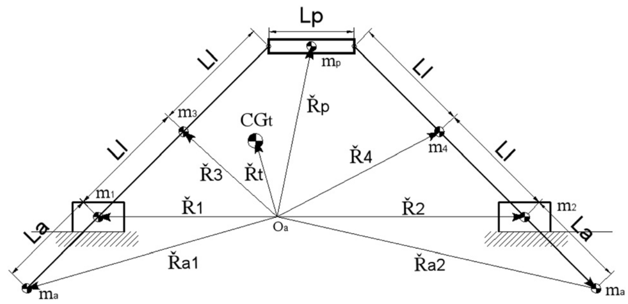


Fig. 6 Mechanism force balancing vector diagram

$$R_t = \frac{1}{M_t}\left(\sum_{i=1}^{N} m_i R_i\right) \tag{28}$$

where $N$ represents the number of mass centers associated with the mechanism.

From Fig. 6, the following vector representation can be expanded utilizing Eq. (28)

$$\begin{aligned} M_t R_t = m_p&\left(R_1 + 2L_l e^{jq_3} + \frac{Lp}{2} e^{j\theta_2}\right) + m_1 R_1 + m_2 R_2 \\ &+ m_3\left(R_1 + L_l e^{jq_3}\right) + m_4\left(R_2 + L_l e^{jq_4}\right) \\ &+ m_a\left(R_1 + L_a e^{j(q_3+\pi)}\right) \\ &+ m_a\left(R_2 + L_a e^{j(q_4+\pi)}\right) \end{aligned} \tag{29}$$

where

$$R_1 = \left(L_q + q_1\right)e^{j\theta_1}, \quad R_2 = \left(L_q + q_2\right)e^{j\theta_2}, \quad \theta_1 = \pi, \text{ and } \theta_2 = 0$$

It is clear from Eq. (29) that the mechanism used in this study cannot be completely force balanced by this methodology for any values of the counterweight mass and length. This is an expected result. However, this mechanism does possess some properties that can allow for a simple analytical solution for a unidirectional force balance. This is illustrated below.

Unidirectional force balancing of parallel mechanisms has been previously achieved by elastic compensation [18], in which springs or elastic elements are used to keep the potential energy of the system constant for all configurations. However, the practicality of using elastic element for such a purpose has not yet been addressed. In this study regarding Re-Dyn, if dynamic force balancing is a requirement, it is chosen to utilize the traditional counterweight method. The 2DOF case study is shown to provide the same unidirectional balancing properties. This is achieved by analyzing Eq. (29) and taking only the terms associated with the passive joint angles, $q_3$ and $q_4$, for conditioning. This conditioning refers to analyzing the set conditions that may force the global manipulator mass center to not vary with any given set of the passive joint angles. With this, the linear momentum in the vertical (gravitational) direction will be eliminated thus eliminating any reaction force in the same direction. With this goal in mind the terms in Eq. (29) that are associated with the passive joint variables are given by

$$e^{jq_3}\left(2m_p L_l + m_3 L_l + m_a L_a e^{j\pi}\right) \tag{30}$$

and

$$e^{jq_4}\left(m_4 L_l + m_a L_a e^{j\pi}\right) \tag{31}$$

Since the mass of both links 3 and 4 are equal and the counterweights mass and length are equal, forcing the above two equations to zero requires use of one of the mechanisms properties. The planar motion of the mechanism exhibits a relationship between the passive joint angles. This relationship is simply $q_4 = \pi - q_3$ for any configuration. Utilizing this relationship, Eqs. (30) and (31) can be combined and the component affecting vertical movement of the mass center can be extracted. This is given by

$$\sin(q_3)\left(2m_p L_l + m_3 L_l - m_a L_a\right) + \sin(q_3)\left(m_4 L_l - m_a L_a\right) = 0 \tag{32}$$

which is easily solvable.

From the above analysis, the unidirectional force balancing of the parallel mechanism can be achieved while holding the following relationship true:

$$L_a = \frac{L_l}{m_a}\left(m_p + m_3\right) \tag{33}$$

For the purpose of measuring the inequality of the above equation, the following is defined in this study

$$\zeta = \left| L_a - \frac{L_l}{m_a}\left(m_p + m_3\right)\right| \tag{34}$$

where the closer $\zeta$ is to zero the closer to perfect balancing the mechanism is.

## 6 Dynamic Performance

The performance of parallel manipulators in the flexible manufacturing regime is composed of several aspects. These aspects many times are dependent on the type of use of the PM. In particular, when the application requires high speeds, the effect of the manipulator dynamics plays an essential role. Its dynamic performance can govern energy consumption, pose accuracy and stability among others. Consequently, the dynamic study of PMs is essential. A brief performance study of the nominal version of the PM used in this study was conducted by the authors in Ref. [38], where the below performance index was derived. Dynamic performance indication is utilized in the proposed Re-Dyn method, and is consequently presented here.

**6.1 Derivation of the Performance Index.** Fundamentally, in the regime of parallel robotics some kinematic properties inherently affect the dynamic performance. As a consequence, it is useful to incorporate a kinematic performance measure coupled with a dynamic measure.

By rewriting Eq. (9) in incremental form, an approximation that maps the active joint errors to the end effector pose errors is attained as

$$\Delta X = J_q(q)\Delta q_q \tag{35}$$

where the forward Jacobian matrix, $J_q(q)$, can also be obtained by $J_x^{-1}(x, y)$.

Consequently, the condition number of the Jacobian matrix [39] can be formulated by

$$\kappa = \left\|J_q^{-1}\right\|_2 \left\|J_q\right\|_2, \quad 1 \le \kappa \le \infty \tag{36}$$

where $\|\bullet\|_2$ indicates the second norm of the matrix.

In the above relation a condition number of $\kappa = 1$ represents a kinematically isotropic condition in which the active joint error, $\Delta q_q$, is not amplified, and the situation when $\kappa = \infty$ represents a singularity and an infinite amplification of the joint error, $\Delta q_q$. Thus, utilizing this kinematic condition, one can avoid singular points as well as give an indication of possible pose errors in a control situation.

Rewriting the dynamic Eq. (26) after neglecting the terms not directly associated with acceleration, the following relationship is arrived at

$$M(q)\ddot{q}_a = \tau_a \tag{37}$$

where

$$M(q) = J_e^T\left\{\left(\sum_{i=1}^{K} J_i^T M_i J_i\right) J_e\right\}$$

Subsequently, the minimum ($\sigma_{\min}$) and maximum ($\sigma_{\max}$) singular values of the inertia matrix above can be determined. The dynamic index in this study is defined as

$$\gamma = \sigma_{\min}/\sigma_{\max} \tag{38}$$

where the larger the value of $\gamma$ the more dynamically isotropic the performance will be.

Utilizing the combined properties of the above two described indices, a performance index can be defined as the weighted combination. This is given by

$$\psi = w_1\gamma + w_2\frac{1}{\kappa} \tag{39}$$

where $w_1$ and $w_2$ are the weights associated with either of the terms.

## 7 Re-Dyn Methodology

In this section, the main idea of this manuscript is presented and a method termed Re-Dyn is proposed. This method is aimed at the flexible manufacturing regime. It encompasses a design change to PMs that enables some of their dynamic properties to be reconfigured. This reconfiguration then allows the manipulator to perform optimally for a multitude of requirements or tasks that are predefined.

**7.1 Re-Dyn Formulation.** The primary objective of the Re-Dyn method is to design a parallel manipulator with reconfigurable dynamics. This method falls into the category of dimensional synthesis and can be a way to determine the amount of kinematic and dynamic reconfiguration needed to satisfy multiple requirements. That is, how much shall the designer physically make the kinematic and dynamic parameters change.

*7.1.1 Re-Dyn.* The systematic procedure for Re-Dyn for flexible manufacturing is as follows. Given the general topology of the mechanism structure, its kinematics and dynamics are derived. Subsequently, the following steps encompass the method:

(1) The design variables are obtained by analyzing $||J_i||$ of each of the connected bodies.
(2) Determine the specifications of the FRs in task space.
(3) The designer now chooses the performance indicators linked to the FRs (e.g., stiffness, reaction forces, dynamic actuator forces).
(4) A multitude of optimization problems are set up. These correspond to a mapping from each functional task space to design space.
(5) The optimization sequences are solved and the results are compiled in a vector of design variable solutions $\mathrm{DV}_i$, corresponding to the $i$th variable. Then the maximum (max) and minimum (min) values are taken for each variable. This is given by $\min(\mathrm{DV}_i), \max(\mathrm{DV}_i)$.

The above constitutes the Re-Dyn method and results in the bounds on the reconfigurable variables needed to fulfill all the requirements optimally. It is worth noting that during step 1, it is proposed to use the link Jacobians to find appropriate design variables. Once the dynamics has been formulated with the connection method, each $J_i$ can reveal which parameters (kinematic and dynamic) affect the motion of the mass centers more so. This eliminates any intuitive need to select the parameters. Consequently, the amount of design variables can be minimized.

**7.2 Performance Design.** In this section, the mapping from DPs to FRs is theoretically described. Also, step 4 of the proposed method is formulated in an objective function for convenience to the reader.

A mapping from functional space to design space has been described by the fundamentals of the Axiomatic design principles [40].

This can be described as a mapping from the FR directly to the DP. In general, the design parameters will be subject to a set of constraints determined directly by the behavior of the functional requirements.

All of the functional requirements come from the manufacturing process or the task space of the robot. These will always be a set of multiple requirements for the PM and may consist of several foreseen tasks that the robot must perform in a flexible manufacturing situation. A design matrix that encompasses a representation of the mapping of the functional requirement space onto the design parameter space can be represented in general form as follows:

$$\begin{bmatrix} \mathrm{FR}_1 \\ \mathrm{FR}_2 \\ \vdots \\ \mathrm{FR}_n \end{bmatrix} = \begin{bmatrix} x & \cdots & \cdots & \vdots \\ \vdots & x & \cdots & \vdots \\ \vdots & \cdots & x & \vdots \\ \vdots & \cdots & \cdots & x \end{bmatrix} \begin{bmatrix} \mathrm{DP}_1 \\ \mathrm{DP}_2 \\ \vdots \\ \mathrm{DP}_n \end{bmatrix} \tag{40}$$

where $n$ is the total number of functional requirements.

In a problem such as one in the manufacturing regime, the design parameters are likely highly coupled between functional requirements as evident by the full matrix, which theoretically will have a rank of 1.

Step 4 of the Re-Dyn method can be formulated as a general optimization problem. Consequently, it is solvable by various methods. Let the dynamic performance parameter be represented by $D_I \in R^R$. Then design objective of this approach can be formulated as

$$D_I = \sum_{i=1}^{r} (\phi_i|\gamma_i| + \chi_i|\eta_i|) \tag{41}$$

where $\phi_i$ and $\chi_i$ are weighting factors for each component determined by the designer for suitability. $\gamma_i$ and $\eta_i$ are the functions directly associated with the dynamic performance from the designer's discretion in step 3.

## 8 Design Study Example With Re-Dyn

The Re-Dyn approach formulated above is for the general case. In this section, the approach is applied to the PM detailed in the first part of the manuscript.

The first step in generating a robotic manipulator that has Re-Dyn properties is to select the design variables. As outlined in sec. 7, the link Jacobians are utilized in this step because they describe how the mass centers can change with time. These are derived using Eq. (23) and are detailed for the specific PM just below Eq. (25). If the two-norm of the link Jacobians are taken, it is evident that the top influential physical parameters that will affect its magnitude are the mass $m_a$, the length $L_a$ and the length $L_1$. These are the same parameters that affect the magnitude of the individual elements of the Jacobians. Notably, the mass $m_3$ will also have an effect. However, it is coupled with $m_a$ and is deemed less practical to be reconfigured and thus not included as a design variable. A simplistic model of the PM with dynamically reconfigurable parameters is given in Fig. 7.

The next step in the formulation is determining the specifics for the functional requirements. Essentially, this would be enough specifications to solve the dynamic model. Suppose that the functional requirements for a parallel robotic mechanism consist of conducting a specified industrial task, or even a multitude of tasks. These tasks are different tasks, such as two or more fast pick and place operations from one spot to another or a couple machining operations on a part.

Two tasks are chosen to illustrate the design process. The tasks consist of two different trajectory maps for the manipulator in different positions in a general large task workspace. For simplicity, the end effector relative trajectory will be the same between the tasks but the placement in the workspace will be different in order

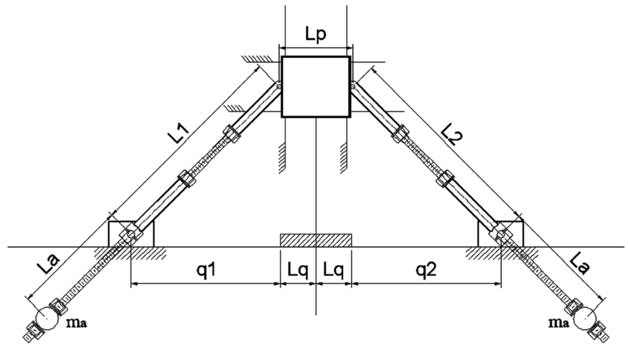


**Fig. 7 Parallel robot with Re-Dyn properties**

to simulate variations in tasks. Consequently, the functional requirement consists of tracking an elliptical shaped end effector trajectory. This can be formulated as

FR1: Tracking an elliptical end effector trajectory with center (0,1.5), radius $y$: 0.25, radius $x$:0.05, at 2 Hz
FR2: Tracking an elliptical end effector trajectory with center (0,3), radius $y$: 0.25, radius $x$:0.05, at 2 Hz

where, radius x and radius y are the x and y coordinate radii, respectively.

The third step is to choose the dynamic performance indicators that are linked to the FRs. For this case study, the dynamic performance measures are those derived in sections 5 and 6. These are detailed and given by Eqs. (39) and (34). The forth step is to formulate the general optimization problem. For this PM, a general addition of the indices is used, which yields a design objective

$$D_l = \psi + \zeta \tag{42}$$

that is specific to the performance indices chosen by the designer.

The final step is to determine the bounds on reconfiguration for each of the design variables. This is outlined below with corresponding details regarding optimization constraints.

### 8.1 Inequality Design Constraints.

Corresponding to the fifth and last step of the procedure, an optimization problem must be solved. In general, the optimization formulation is subject to constraints that are fundamental to robotic system design. Each design variable is subject to upper and lower bounds set by the designer. Also, the robot must remain within its workspace bounded by singularities. This is achieved by constraining variables while utilizing a singularity analysis of the forward and inverse kinematics of the manipulator.

**Table 1 Fundamental parameters; for reconfigurability optimization**

| Parameters | Values |
|---|---|
| $m_p$ (kg) | 20 |
| $m_3$ (kg) | 13 |
| $m_q$ (kg) | 7 |
| $L_q$ (m) | 0.1 |
| $L_p$ (m) | 0.3 |

**Table 2 Optimization results corresponding to each FR**

| FR# | $L_1$ (m) | $m_a$ (kg) | $L_a$ (m) |
|---|---|---|---|
| 1 | 2.3937 | 14.6392 | 2.698 |
| 2 | 4.526 | 12.5098 | 5.9696 |

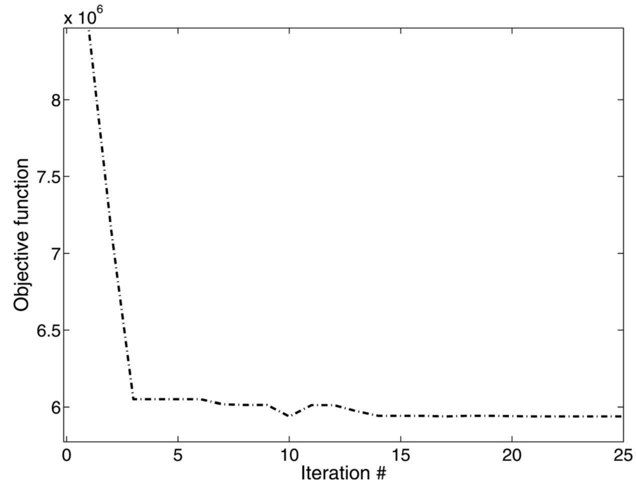


**Fig. 8 Objective function convergence**

### 8.2 Results of the Re-Dyn Variables.

The objective function setup in step 4 is then optimized. This optimally maps the task space to design space for each FR. The optimization problem in this study has no analytical solution due to its high complexity. Consequently, the Sequential Simplex method has been programmed and utilized. Notably, any optimization scheme can be used or customized in this step of the proposed method. The fundamental parameters that correspond to the PM used as a case study are compiled in Table 1. The optimization procedure is conducted and the optimal values for each task space or FR is given in Table 2 for convenience. And an example of the convergence of one of the optimization schemes can be observed in Fig. 8. The following vectors of design solutions are eventually obtained:

$$\mathrm{DV}_1 = [\,2.3937 \quad 4.5260\,] \tag{43a}$$

$$\mathrm{DV}_2 = [\,14.6392 \quad 12.5098\,] \tag{43b}$$

$$\mathrm{DV}_3 = [\,2.6980 \quad 5.9696\,] \tag{43c}$$

to which taking $\min(\mathrm{DV}_i), \max(\mathrm{DV}_i)$ constitutes the last part of step 5. This also yields the bounds on the reconfigurability for each design variable.

Thus, the parallel robot utilized in this study must have its kinematic and inertial mass properties reconfigurable with bounds encompassing that of the optimal results. This is the requirement set for the physical parameters.

## 9 Control and Dynamic Force Simulations

This section focuses on simulating the parallel robot under forward dynamic situations. Namely, the simulations focus on the situation in which the robot is conducting the function tasks it was designed for. Though control is utilized in this section in order to characterize performance situations, it is not the focus of this case study. Thus, a linear proportional derivative control sequence with fixed parameters for all simulations is used, for comparison purposes.

This section is set out to compare simulation results whilst the robot is conducting FR1 and FR2 to that of another robot that does not have the prescribed kinematic and dynamic properties reconfigurable. This standard robot is termed the nominal robot in this study. It is a robot with the same topology of the Re-Dyn PM that simply has a longer leg length of 7 m ($L_1 = L_2 = 7$ m) so that its workspace may encompass multiple functional requirements. It also does not have the added components for force balancing

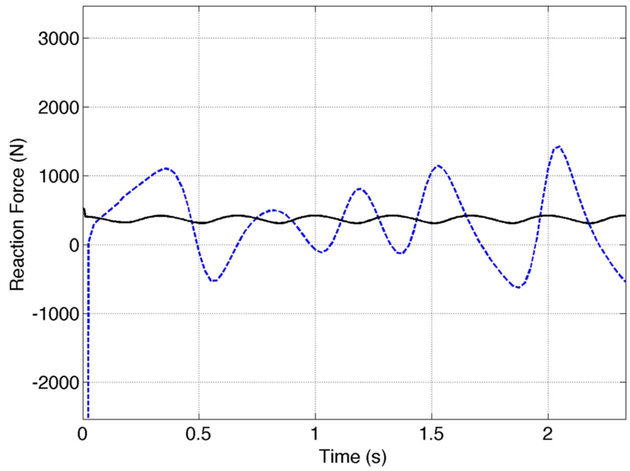


**Fig. 9 FR1, Nominal (dashed) versus dynamically reconfigured (solid), reaction force**

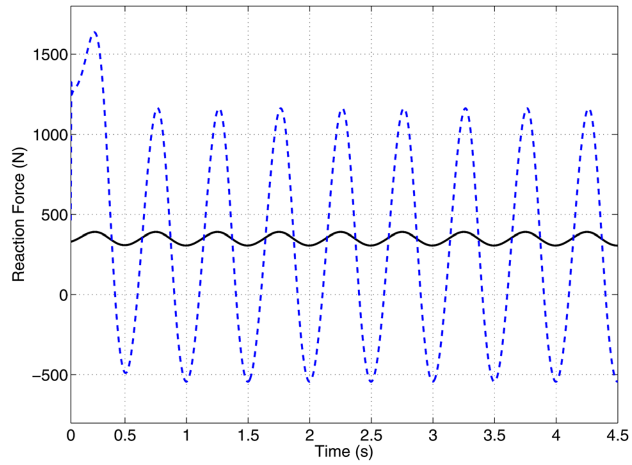


**Fig. 10 FR2, Nominal (dashed) versus Re-Dyn (solid), reaction force**

($L_a = m_a = 0$). All other parameters remain the same as the Re-Dyn robotic structure. In this section, the forward dynamics was simulated with Simulink and SimMechanics at a tracking frequency of 2 Hz. This was appropriate because the model could also be utilized to calculate reaction forces and develop a control loop.

The results for the reaction force for the first FR is illustrated in Fig. 9, while the computed root mean square (RMS) error and offset error are given in Tables 3 and 4 for the nominal system and the proposed system respectively. While the proposed robot conducts a stable tracking situation using the fixed parameter controller, the nominal system in this case was not stable in this region of its workspace for the latter part of the simulation with the same controller. The control effort was not sufficient enough to provide tracking for this functional requirement, consequently its end effector passed through a singular region just after 2 s of simulation. It is thought that a more complex controller should be able to provide tracking in this region. For illustration purposes, its reaction forces during the time that it remained stable is shown in Fig. 9. Evidently, the reaction force of the nominal system is much larger than that of the Re-Dyn robotic system. For the second functional requirement, both robots remained stable and tracked the functional requirement while attaining satisfactory results. The results for the reaction force can be observed in Fig. 10. The nominal system produced a very large reaction force, whereas the Re-Dyn one produces a very slight oscillatory force as expected. The corresponding results for the control errors can be observed in Table 3. While comparing the nominal robot to the proposed one, the RMS error is similar and the average offset error is more than 60 times less for the Re-Dyn system. This indicates that whilst the Re-Dyn robot has extra components for force balancing, its reconfigurability allows it to perform better than the nominal robot in a forward dynamic situation when conducting its

**Table 3 Nominal robot, control errors for both FRs (the subscripts 1 and 2 refer to FR1 and FR2, respectively**

| $\text{RMS}_1$ | $\text{RMS}_2$ | Offset $\text{error}_1$ | Offset $\text{error}_2$ |
|---|---|---|---|
| unstable | 0.0135 | unstable | −0.0068 |

**Table 4 Re-Dyn robot, control errors for FR1 and FR2**

| $\text{RMS}_1$ | $\text{RMS}_2$ | Offset $\text{error}_1$ | Offset $\text{error}_2$ |
|---|---|---|---|
| 0.0234 | 0.0129 | −0.0069 | −0.001 |

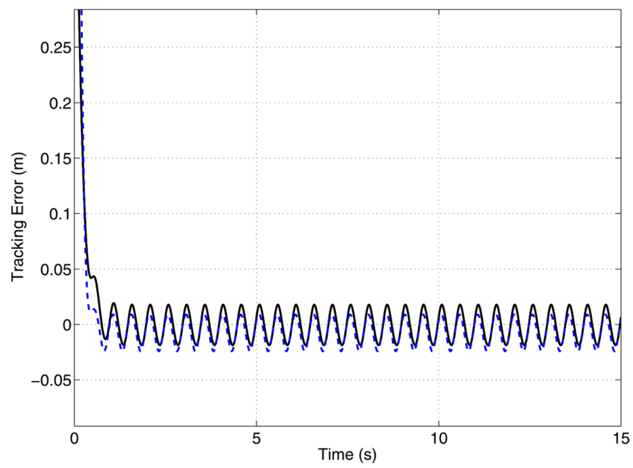


**Fig. 11 FR2, tracking error, nominal (dashed), Re-Dyn (solid)**

functional requirement number 2. Also, it performed well for the first functional requirement, while the nominal robot failed after 2 s.

Also, during the simulations, the resulting tracking errors were collected and compared for the nominal robot and the Re-Dyn one for FR2. These correspond to the data utilized for the computations of Tables 3 and 4. The time data can be observed in Fig. 11. The tracking errors observed in Fig. 11 confirm the data of Tables 3 and 4. Also, the control effort was measured during simulations. Figure 12 illustrates the control effort comparing the nominal robot to the Re-Dyn one for FR2. Evidently, the Re-Dyn robot will consume slightly more energy, which is expected due to its added masses which are also reconfigurable. Notably, the control effort peak for the two robots was approximately the same. This in turn indicates the same actuators can be utilized between the two robots. The optimal compromise between reaction force and control effort can also be changed by the designer in step 3 of the Re-Dyn method by either changing the indices or inducing more weight on a term. Since the mass for a robot that has Re-Dyn is changeable as well as removable, it is valid to even change performance indices between FRs.

Notably, these simulations show that reconfiguring the kinematic and dynamic properties of the robot can potentially make use of one robot with good dynamic characteristics for multiple tasks, which would not be possible with one traditional robotic mechanism. Emphasis is placed on an optimal dynamic

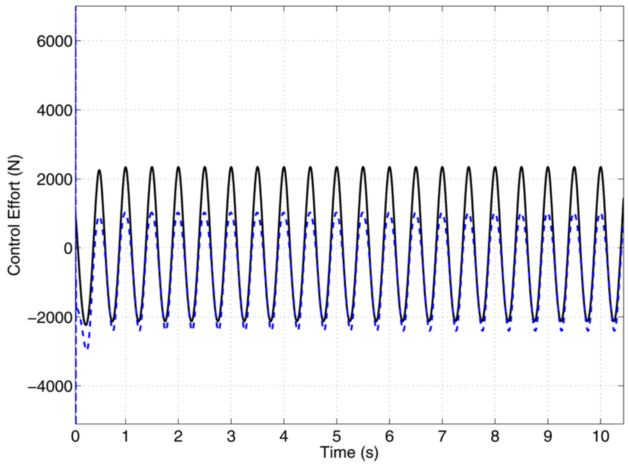


**Fig. 12 FR2, Control effort, nominal (dashed), Re-Dyn (solid)**

configuration for each functional requirement. On a side note, related performance indices for things such as the speed of the robot may also be obtained from the dynamic model. These can be investigated in a future work.

## 10 Conclusions

This work has endeavored into the flexible manufacturing regime where reconfigurable robotic systems will be the future of technological innovations. The idea to synthesize robotic systems with dynamic properties that are reconfigurable is investigated. As a consequence, a method is proposed in a step sequence that enables the optimal design of the parameters of a robot that has its kinematic and dynamic parameters reconfigurable. An example mechanism is studied in detail for this purpose. The study first formulates its kinematics and forward dynamic model. The connection method is utilized. Subsequently, a description of possible performance indices is illustrated in terms of the force balancing and dynamic performance. The Re-Dyn method is then formulated in the general case which is applicable to any PM for the purpose of flexible manufacturing. It is then applied to the case study robotic structure. Lastly, a simulation study is conducted to illustrate the advantages of the proposed Re-Dyn method.

## Acknowledgment

The authors are grateful for the support received from the Canada Research Chairs (CRC) program, the Natural Sciences and Engineering Research Council of Canada (NSERC) and Ontario Graduate Scholarship (OGS). The authors are also grateful for the input from the anonymous reviewers.

## References

[1] Li, Y., Wang, J., Liu, X.-J., and Wang, L.-P., 2010, "Dynamic Performance Comparison and Counterweight Optimization of Two 3-DOF Parallel Manipulators for a New Hybrid Machine Tool," Mech. Mach. Theory, **45**(11), pp. 1668–1680.
[2] Miller, K., 2004, "Optimal Design and Modeling of Spatial Parallel Manipulators." Int. J. Rob. Res., **23**(2), pp. 127–140.
[3] Sugimoto, K., 1987, "Kinematic and Dynamic Analysis of Parallel Manipulators by Means of Motor Algebra," J. Mech., Transm., Autom. Des., **109**(1), pp. 3–7.
[4] Lee, K. M., and Shah, D. K., 1988, "Dynamic Analysis of a Three-Degrees-of-Freedom in-Parallel Actuated Manipulator," IEEE J. Rob. Autom., **4**(3), pp. 361–367.
[5] Wu, J., Wang, J., Li, T., Wang, L., and Guan, L., 2008, "Dynamic Dexterity of a Planar 2-DOF Parallel Manipulator in a Hybrid Machine Tool," Robotica, **26**(1), pp. 93–98.
[6] Kane, T., and Levinson, D., 1985, *Dynamics, Theory and Applications*, McGraw-Hill, New York.
[7] Huang, Q., Haadeby, H., and Sohlenius, G., 2002, "Connection Method for Dynamic Modelling and Simulation of Parallel Kinematic Mechanism (PKM) Machines," Int. J. Adv. Manuf. Technol., **19**, pp. 163–173.
[8] Qi, H., Liwen, G., Jinsong, W., and Liping, W., 2010, "GA-Based Dynamic Manipulability Optimization of a 2-DOF Planar Parallel Manipulator," 2010 IEEE Conference on Robotics Automation and Mechatronics (RAM), pp. 46–51.
[9] Zhao, Y., and Gao, F., 2009, "Dynamic Formulation and Performance Evaluation of the Redundant Parallel Manipulator," Rob. Comput.-Integr. Manufact., **25**, pp. 770–781.
[10] Dasgupta, B., and Mruthyunjaya, T., 1998, "A Newton-Euler Formulation for the Inverse Dynamics of the Stewart Platform Manipulator," Mech. Mach. Theory, **33**(8), pp. 1135–1152.
[11] Zhang, C.-D., and Song, S.-M., 1993, "An Efficient Method for Inverse Dynamics of Manipulators Based on the Virtual Work Principle," J. Rob. Syst., **10**(5), pp. 605–627.
[12] Tadokoro, S., Kimura, I., and Takamori, T., 1991, "A Measure for Evaluation of Dynamic Dexterity Based on a Stochastic Interpretation of Manipulator Motion," Fifth International Conference on Advanced Robotics, 1991, Robots in Unstructured Environments, 91 ICAR, Vol. 1, pp. 509–514.
[13] Gregorio, R. D., and Parenti-Castelli, V., 2005, "On the Characterization of the Dynamic Performances of Planar Manipulators," Meccanica, **40**, pp. 267–279.
[14] Wang, L. P., Wang, J. S., and Chen, J., 2005, "The Dynamic Analysis of a 2-PRR Planar Parallel Mechanism," Proc. Inst. Mech. Eng., Part C: J. Mech. Eng. Sci., **219**(9), pp. 901–909.
[15] Wu, J., Wang, J., Wang, L., and Li, T., 2009, "Dynamics and Control of a Planar 3-DOF Parallel Manipulator With Actuation Redundancy," Mech. Mach. Theory, **44**(4), pp. 835–849.
[16] Jiang, Q., and Gosselin, C. M., 2010, "Dynamic Optimization of Reactionless Four-Bar Linkages," ASME, J. Dyn. Syst., Meas., Control, **132**(4), p. 041006.
[17] Gosselin, C. M., Vollmer, F., Cote, G., and Wu, Y., 2004, "Synthesis and Design of Reactionless Three-Degree-of-Freedom Parallel Mechanisms," IEEE Trans. Rob. Autom., **20**(2), pp. 191–199.
[18] Carricato, M., and Gosselin, C., 2009, "A Statically Balanced Gough/Stewart-Type Platform: Conception, Design, and Simulation," J. Mech. Rob., **1**(3), p. 031005.
[19] Briot, S., Bonev, I. A., Gosselin, C. M., and Arakelian, V., 2009, "Complete Shaking Force and Shaking Moment Balancing of Planar Parallel Manipulators With Prismatic Pairs," Proc. Inst. Mech. Eng., Part K: J. Multi-Body Dyn., **223**(1), pp. 43–52.
[20] Alici, G., and Shirinzadeh, B., 2004, "Optimum Dynamic Balancing of Planar Parallel Manipulators," IEEE International Conference on Proceedings of Robotics and Automation, ICRA'04, Vol. 5, IEEE, pp. 4527–4532.
[21] Fattah, A., and Agrawal, S. K., 2006, "On the Design of Reactionless 3-DOF Planar Parallel Mechanisms," Mech. Mach. Theory, **41**(1), pp. 70–82.
[22] Wu, Y., and Gosselin, C., 2005, "Design of Reactionless 3-DOF and 6-DOF Parallel Manipulators Using Parallelepiped Mechanisms," IEEE Trans. Rob., **21**(5), pp. 821–833.
[23] Van der Wijk, V., and Herder, J. L., 2009, "Synthesis of Dynamically Balanced Mechanisms by Using Counter-Rotary Countermass Balanced Double Pendula," ASME, J. Mech. Des., **131**(11), p. 111003.
[24] Lee, T. W., and Cheng, C., 1984, "Optimum Balancing of Combined Shaking Force, Shaking Moment, and Torque Fluctuations in High-Speed Linkages," ASME J. Mech., Transm. Autom. Des., **106**, pp. 242–251.
[25] Ouyang, P. R., and Zhang, W. J., 2005, "Force Balancing of Robotic Mechanisms Based on Adjustment of Kinematic Parameters," ASME, J. Mech. Des., **127**(3), pp. 433–440.
[26] Hong, B., and Erdman, A. G., 2005, "A Method for Adjustable Planar and Spherical Four-Bar Linkage Synthesis," ASME, J. Mech. Des., **127**(3), pp. 456–463.
[27] Park, J. H., and Asada, H., 1994, "Concurrent Design Optimization of Mechanical Structure and Control for High Speed Robots," ASME, J. Dyn. Syst., Meas., Control, **116**(3), pp. 344–356.
[28] Pil, A. C., and Asada, H. H., 1996, "Integrated Structure/Control Design of Mechatronic Systems Using a Recursive Experimental Optimization Method," IEEE/ASME Trans. Mechatron., **1**(3), pp. 191–203.
[29] Li, Q., Zhang, W. J., and Chen, L., 2001, "Design for Control-A Concurrent Engineering Approach for Mechatronic Systems Design," IEEE/ASME Trans. Mechatron., **6**(2), pp. 161–169.
[30] Li, Q., and Wu, F. X., 2004, "Control Performance Improvement of a Parallel Robot Via the Design for Control Approach," Mechatronics, **14**(8), pp. 947–964.
[31] Ouyang, P. R., Li, Q., and Zhang, W. J., 2003, "Integrated Design of Robotic Mechanisms for Force Balancing and Trajectory Tracking," Mechatronics, **13**(8–9), pp. 887–905.
[32] McGovern, J., and Sandor, G. N., 1973, "Kinematic Synthesis of Adjustable Mechanisms, Part 1: Function Generation," ASME Mechanisms Conference, pp. 417–422.
[33] McGovern, J., and Sandor, G. N., 1973, "Kinematic Synthesis of Adjustable Mechanisms, Part 2: Path Generation," ASME Mechanisms Conference, pp. 423–429.
[34] Chuenchom, T., and Kota, S., 1994, "Analytical Synthesis of Adjustable Dyads and Triads for Designing Adjustable Mechanisms," Proceedings of the ASME Design Technical Conference, Vol. 70, pp. 467–477.
[35] Bi, Z., and Wang, L., 2009, "Optimal Design of Reconfigurable Parallel Machining Systems," Rob. Comput.-Integr. Manufact., **25**(6), pp. 951–961.
[36] Peng, C., 2010, "Optimal Synthesis of Planar Adjustable Mechanisms," Ph.D. thesis, New Jersey Institute of Technology, Newark, NJ.
[37] Dai, J., Huang, Z., and Lipkin, H., 2006, "Mobility of Overconstrained Parallel Mechanisms," ASME, J. Mech. Des., **128**(1), pp. 220–229.
[38] Coppola, G., Zhang, D., Liu, K., and Gao, Z., 2012, "Dynamic Performance With Control of a 2-DOF Parallel Robot," ASME IDETC/CIE.
[39] Gosselin, C., 1988, "Kinematic Analysis, Optimization and Programming of Parallel Robotic Manipulators," Ph.D. thesis, McGill University, Montreal, Québec.
[40] Suh, N. P., 2001, *Axiomatic Design: Advances and Applications* (The Oxford Series on Advanced Manufacturing), Oxford University Press, New York, NY.